Supplemental Methods

Cell culture and transfection. HEK293, COS7, BOSC23, and SW480 cells are maintained routinely in our laboratory. B16 cells were obtained from the Cell Resource Center for Biomedical Research, Tohoku University (Sendai, Japan), and CHO cells were purchased from American Type Cell Collection (Manassas, VA). HEK293, COS7, BOSC23, SW480, and B16 cells were cultured in DMEM (Nissui) supplemented with 10% FBS and antibiotics. CHO cells were cultured in Ham's F12 medium supplemented with 10% FBS and antibiotics. Cell culture under low glucose conditions was performed with glucose-free DMEM (Invitrogen) supplemented with PBS-dialyzed FBS and the indicated concentrations of glucose. Cell culture under hypoxic conditions was performed using a multi-gas incubator (MCO-5M, SANYO). Expression plasmids and siRNAs were transfected in each cell with LipofectAmine2000 (Invitrogen), unless otherwise noted.

Generation of cell lines stably expressing PRL. Cell lines stably expressing PRL were generated according to the previous studies (1–3), with minor modifications. Briefly, expression plasmids for WT or various mutant forms of PRL were co-transfected with pTK-Hyg into SW480, B16, or CHO cells. Single colonies were isolated after 2–3 weeks of hygromycin selection (200–600 μg/ml), and protein expression was confirmed by immunoblotting.

RNAi knockdown. For transient knockdown experiments, we transfected HEK293 cells with duplex siRNAs against human CNNM4 and PRL-1 purchased from Invitrogen,

which targets the following sequences: *CNNM4*-siRNA (#1), 5′-GCGAGAGCAUGAAGCUGUAUGCACU-3′, *CNNM4*-siRNA (#2), 5′-CCGCCAUUACCUGUACACCCGAAAU-3′, *PRL1*-siRNA (#1), 5′-GCAACUUCUGUAUUUGGAGAAGUAU-3′, and *PRL1*-siRNA (#2), 5′-CCAACCAAUGCGACCUUAAACAAAU-3′. As a control, we used an siRNA that possesses a scrambled sequence of *CNNM4*-siRNA (control siRNA (#1)), 5′-GCGACGAAAGUGUCGGUAUCGAACU-3′ and a non-targeting siRNA sequence (negative control LO GC from Invitrogen, control siRNA (#2)). Stable knockdown in B16 and CHO cells was achieved by expressing shRNA using retroviral infection, as described previously (1). Briefly, we inserted the oligonucleotides, including the following target sequence for mouse *Cnnm4*, 5′-GGAACTGAGAAGGAGAGAA-3′, mouse *Cav2*, 5′-CCTCAGACATTAGAGTAATTT-3′, and hamster *Cnnm4*, 5′-GCTCAGCTTCCCTCAGTTA-3′ (#1) and 5′-GGAAACGGGTATCTATGAA-3′ (#2) into the pSUPER-retro vector (OligoEngine). For control transfections, we used the oligonucleotides including the following scrambled sequence, 5′-GGAAAGCTAGGAAGAGAGA-3′ (#1) and 5′-GGAACTAGAGGAGAGAGAA-3′ (#2). To generate recombinant retroviruses, we co-transfected BOSC23 cells with the pSUPER-retro vector and pCL-ampho packaging vector (Imgenex) with FuGENE6 (Roche), and the culture supernatants containing recombinant retroviruses were used to infect B16 and CHO cells. The cells resistant to treatment with 5 μg/ml puromycin for 48 h were selected.

Identification of PRL-interacting proteins by mass spectrometry. The lysates from SW480 colorectal cancer-derived cells stably expressing FLAG-PRL-1 were subjected

to anti-FLAG immunoprecipitation. Precipitated proteins were separated by SDS-PAGE and visualized by silver staining using the SilverQuest Silver Staining Kit (Invitrogen). The bands of interest were excised from the gel, and the trypsin-digested peptides were subjected to mass spectrometry as described previously (4).

Phosphatase assays. Recombinant His-PRL-3-WT, -C104S, and -C49S proteins were expressed in *E. coli* and purified with Ni-NTA beads (QIAGEN). The purified proteins (0.5 mg/ml) were subjected to phosphatase assays to measure the activity against p-nitrophenyl phosphate (pNPP, 25 mM) as described previously (2). Absorbance at 400 nm (A_{400}), which reflects the concentration of the reaction product, was measured with a plate reader LD400 (Beckman).

Mg^{2+}-imaging analyses with Magnesium Green. Mg^{2+}-imaging analyses with Magnesium Green were performed as described in the previous study (5).

Measurement of $[Mg^{2+}]_i$ with Mag-fura2. HEK293 cells or B16-derived cells were loaded with 2 μM Mag-fura2-AM (Invitrogen) in serum-free DMEM for 45 min at 37°C. The cells were washed once with serum-free DMEM without Mag-fura2. Then, the fluorescence was measured and $[Mg^{2+}]_i$ was subsequently determined as described in the previous study (5).

Direct binding assays. Recombinant proteins of GST and GST-PRL-3 were expressed in *E. coli* and purified with glutathione beads (GE healthcare). CNNM4 proteins were synthesized with a cell-free in vitro system in a liposome-embedded manner, as

described previously (6, 7) and extracted from the liposome using a lysis buffer containing 0.5% Triton X-100. Pull-down assays were performed as previously described (1).

Non-reducing SDS-PAGE. SDS-PAGE under the non-reducing conditions was performed as previously described (8).

RT-PCR analyses. cDNAs were synthesized using total RNAs isolated from HEK293 and B16 cells, as described previously (1). For HEK293-derived cDNA, we used the following primers; *hCNNM1*-fw, 5′-GTCGGAGATCCTGGATGAAA-3′, *hCNNM1*-rv, 5′-ACGTTGGGATGTTTCAGGAG-3′, *hCNNM2*-fw, 5′-CCACCTGGATTTACCACGAC-3′, *hCNNM2*-rv, 5′-CGCTTGGCGTAATTCTTCTC-3′, *hCNNM3*-fw, 5′-GTCGGTTAGGCTGGTTGTTC-3′, *hCNNM3*-rv, 5′-AAGAGGCGCAGGAGGAAG-3′, *hCNNM4*-fw, 5′-CTATACTCGCATCCCGGTGT-3′, and *hCNNM4*-rv, 5′-TCCAACTTGGTGTCATGGAA-3′. The PCR conditions (annealing temperature = 60ºC, 28 cycles) were chosen to prevent DNA amplification from reaching a plateau. As a positive control, we also performed PCR using plasmid vectors containing the cDNA region of each human *CNNM* as templates (6×10^{-14} g). For B16-derived cDNA, we used the following primers to amplify the DNA fragments of mouse CNNMs; *mCnnm1*-fw, 5′-GCCGAGATCTGTCCGTACTC-3′, *mCnnm1*-rv, 5′-GCAGCTTTTCCCTCGTGTAG-3′, *mCnnm2*-fw, 5′-GGAGAACGTTCCAACATCGT-3′, *mCnnm2*-rv,

5′-GCTGTCCGTCTGCTTAAAGG-3′, *mCnnm3*-fw, 5′-CCGGCACTGTCCTAGACTTC-3′, *mCnnm3*-rv, 5′-GCGTCCAGTTTGGTATCGTT-3′, *mCnnm4*-fw, 5′-GCTTCTACAACCACCCGGTA-3′, and *mCnnm4*-rv, 5′-AGCAGCCAGAAGAAGCTGAG-3′. The PCR conditions (annealing temperature = 58ºC, 32 cycles) were similarly standardized to prevent DNA amplification from plateauing. As a positive control, we also performed PCR using plasmid vectors containing the cDNA region of each mouse *Cnnm* as a templates (1×10^{-13} g). We also used the following primers to amplify the DNA fragments of mouse Caveolin-2 and GAPDH, *mCav2*-fw, 5′-ATGACGCCTACAGCCACCACAG-3′, *mCav2*-rv, 5′-GCAAACAGGATACCCGCAATG-3′, *mGapdh*-fw, 5′-TAACATCAAATGGGGTGAGG-3′, and *mGapdh*-rv, 5′-GGTTCACACCCATCACAAAC-3′. The PCR conditions (annealing temperature = 61ºC, 27 cycles) were similarly standardized to prevent DNA amplification from plateauing.

Supplemental References

1. Funato Y, Michiue T, Asashima M, Miki H. The thioredoxin-related redox-regulating protein nucleoredoxin inhibits Wnt-beta-catenin signalling through dishevelled. *Nat Cell Biol.* 2006;8(5):501–508.
2. Diamond RH, Cressman DE, Laz TM, Abrams CS, Taub R. PRL-1, a unique nuclear protein tyrosine phosphatase, affects cell growth. *Mol Cell Biol.* 1994;14(6):3752–3762.
3. Yamaguchi H, Miki H, Takenawa T. Neural Wiskott-Aldrich syndrome protein is involved in hepatocyte growth factor-induced migration, invasion, and tubulogenesis of epithelial cells. *Cancer Res.* 2002;62(9):2503–2509.
4. Nada S, et al. The novel lipid raft adaptor p18 controls endosome dynamics by anchoring the MEK-ERK pathway to late endosomes. *EMBO J.* 2009;28(5):477−489.
5. Yamazaki D, et al. Basolateral Mg^{2+} Extrusion via CNNM4 Mediates Transcellular Mg^{2+} Transport across Epithelia: A Mouse Model. *PLoS Genet.* 2013;9(12):e1003983.
6. Nozawa A, Ogasawara T, Matsunaga S, Iwasaki T, Sawasaki T, Endo Y. Production and partial purification of membrane proteins using a liposome-supplemented wheat cell-free translation system. *BMC Biotechnol.* 2011;11:35.
7. Takai K, Sawasaki T, Endo Y. Practical cell-free protein synthesis system using purified wheat embryos. *Nat Protoc.* 2010;5(2):227–238.
8. Ishii T, Funato Y, Miki H. Thioredoxin-related protein 32 (TRP32) specifically reduces oxidized phosphatase of regenerating liver (PRL). *J Biol Chem.*

2013;288(10):7263–7270.

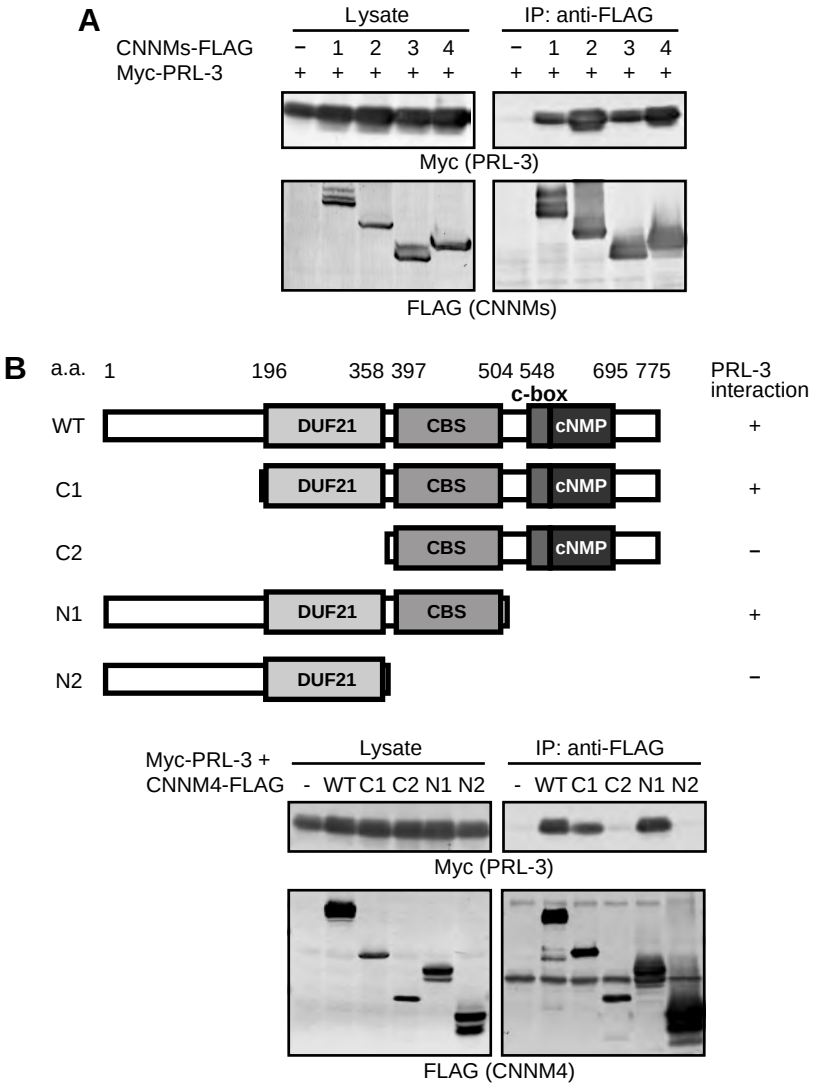

Supplemental Figure 1

Characterization of CNNM–PRL interaction. (**A**) Lysates of COS7 cells transfected with the indicated constructs were subjected to immunoprecipitation with anti-FLAG antibody. The precipitates were analyzed by immunoblotting with the indicated antibodies. (**B**) Top: Schematics of CNNM4 deletion constructs. The number of amino acid residues is indicated. Bottom: Lysates of COS7 cells expressing CNNM4-FLAG (WT and the indicated deletion mutants) and Myc-PRL-3 were subjected to immunoprecipitation with anti-FLAG antibody. The precipitates were analyzed by immunoblotting with the indicated antibodies. Representative immunoblots from 3 independent experiments are shown in each panel.

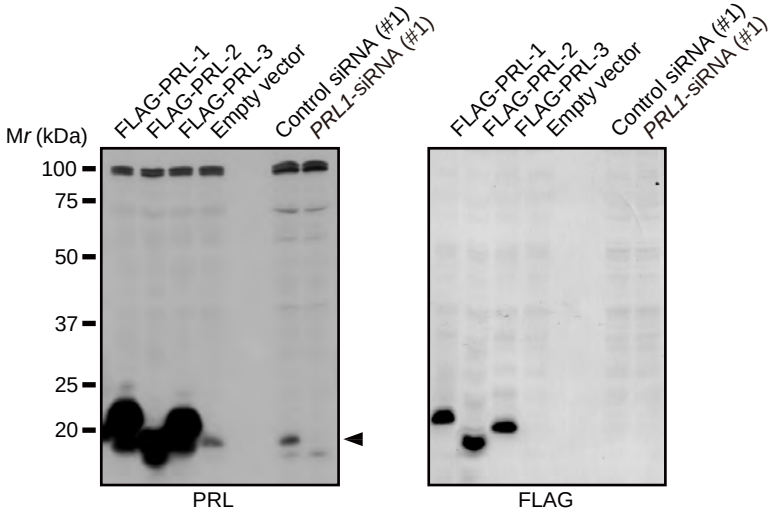

Supplemental Figure 2
Characterization of anti-PRL antibody. Lysates of HEK293 cells transfected with the indicated expression constructs or siRNAs were subjected to immunoblotting analyses with the anti-PRL antibody. The endogenous PRL (mainly PRL-1) signal in HEK293 cells is indicated with an arrowhead. Representative immunoblots from 3 independent experiments are shown.

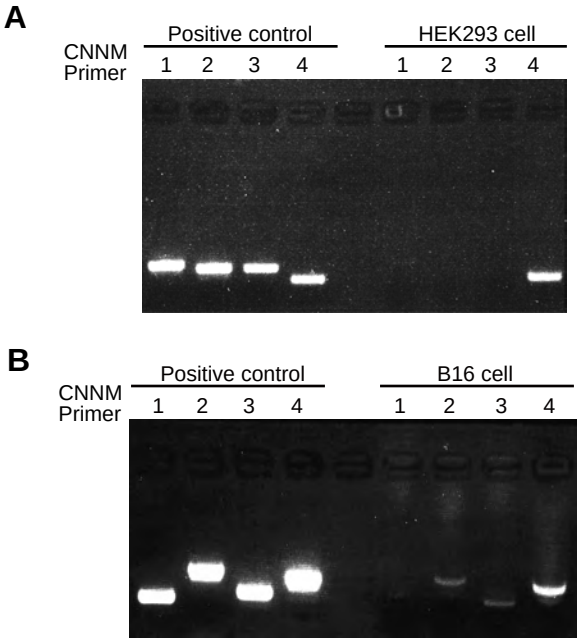

Supplemental Figure 3
RT-PCR expression analyses of the CNNM family. Total RNA was collected from HEK293 cells (A) or B16 cells (B), and RT-PCR analysis was carried out for each CNNM isoform. The PCR results employing each human (A) or mouse (B) CNNM cDNA as a template are also shown as positive controls. Representative gels from 3 independent experiments are shown in each panel.

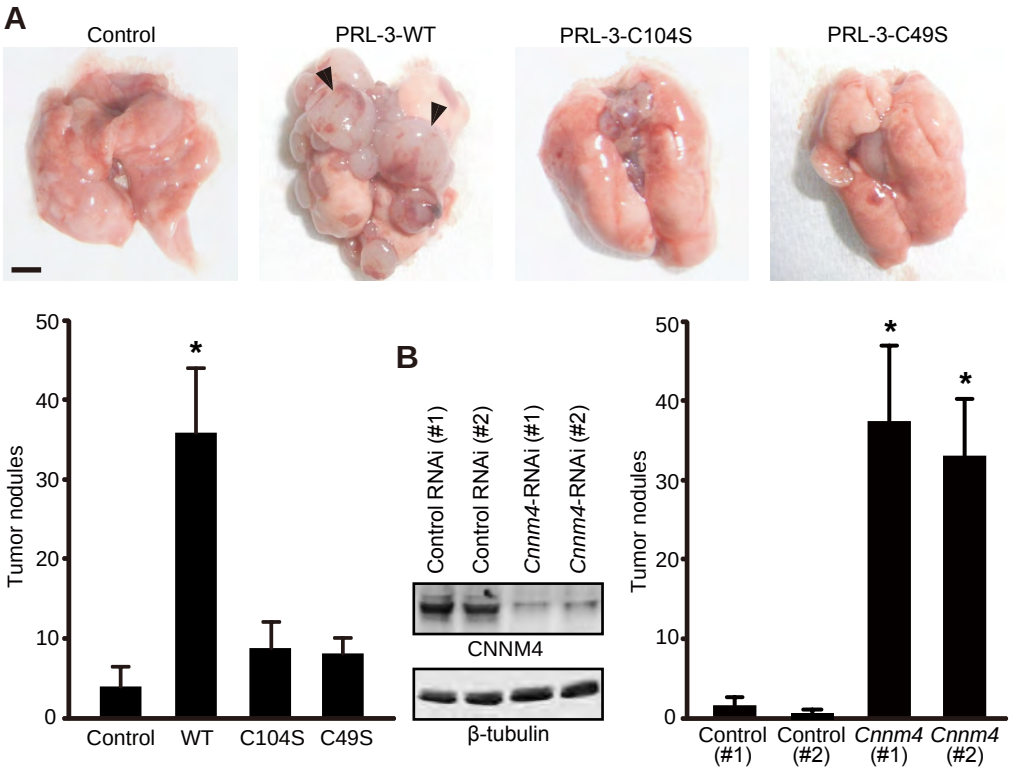

Supplemental Figure 4
PRL promotes tumor growth via CNNM4 in CHO cells. (**A**) CHO cells stably expressing FLAG-PRL-3 were subjected to tumor formation experiments. The numbers of the tumor nodules on the lungs are shown as mean ± SEM (n = 6; 2 independent cell clones for each construct). *p* value was determined by the two-tailed multiple t-test with Bonferroni's correction following ANOVA. *: $p < 0.05$ against control cells. Bar, 2 mm. (**B**) *Cnnm4*-RNAi CHO cells were subjected to tumor formation experiments (mean ± SEM, n = 6; 2 independently obtained cells for each construct). *p* values were determined by the two-tailed multiple t-test with Bonferroni's correction following ANOVA. *: $p < 0.05$ against control RNAi cells (both #1 and #2). Representative immunoblotting results for endogenous CNNM4 (from 3 independent experiments) are also indicated (left).

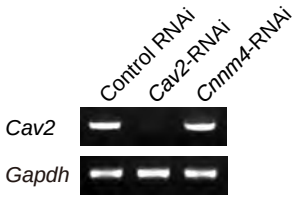

Supplemental Figure 5
RT-PCR analysis of *Cav2*. Total RNA was collected from B16-derived cell lines expressing shRNA against *Cav2* or *Cnnm4*, and RT-PCR analysis of *Cav2* and *Gapdh* was performed. Representative gels from 3 independent experiments are shown.